

УДК 620.9

Doi: 10.31772/2712-8970-2024-25-1-126-142

Для цитирования: Энергетика тангенциального подводящего устройства микротурбины системы терморегулирования перспективного космического аппарата / Ю. Н. Шевченко, А. А. Кишкин, А. А. Зуев и др. // Сибирский аэрокосмический журнал. 2024. Т. 25, № 1. С. 126–142. Doi: 10.31772/2712-8970-2024-25-1-126-142.

For citation: Shevchenko Yu. N., Kishkin A. A., Zuev A. A. et al. [Power engineering of the tangential supply device of the microturbine of the thermal control system of a promising spacecraft]. *Siberian Aerospace Journal*. 2024, Vol. 25, No. 1, P. 126–142. Doi: 10.31772/2712-8970-2024-25-1-126-142.

Энергетика тангенциального подводящего устройства микротурбины системы терморегулирования перспективного космического аппарата

Ю. Н. Шевченко, А. А. Кишкин^{*}, А. А. Зуев, А. В. Делков, Д. А. Жуйков

Сибирский государственный университет науки и технологий имени академика М. Ф. Решетнева
Российская Федерация, 660037, г. Красноярск, просп. им. газ. «Красноярский рабочий», 31

^{*}E-mail: spsp99@mail.ru

В настоящей работе представлен обзор современной технической проблемы, связанной с двухфазными системами терморегулирования космических аппаратов, и возможные технические приложения рекуперации тепловой энергии в органическом цикле Ренкина как составной части систем обеспечения теплового режима. Конструктивное решение подразумевает собой интегрирование паровой микротурбины за радиатором-испарителем. Микротурбина представляет собой тангенциальное подводящее устройство и радиально центrostремительное рабочее колесо низкой быстроходности $n_{st} < 40$. В этой области не существует достоверных данных по проектированию и энергетике как подводящего устройства, так и рабочего колеса. Энергетика (потери энthalпии) подводящего устройства определяет в основном транспорт закрученного потока к рабочему колесу и, как следствие, окружную работу на турбине. Разработан и представлен прототип радиальной микротурбины с целью оценки конструктивного исполнения проточной части как подводящего устройства, так и рабочего колеса. В результате анализа выделены основные определяющие гидродинамические участки, необходимые для гидродинамического анализа и математической проработки алгоритма расчета течений с оценкой энергетических потерь: течение закрученного потока радиально-кольцевой щели; осе-кольцевой щели и тангенциального подводящего устройства. Первые два алгоритма предполагают расчетное моделирование. Модель энергетических потерь в тангенциальном подводящем устройстве не поддается аналитическому моделированию, поскольку включает в себя последовательность (или совместность) течения в граничных условиях, определяемых как «местные сопротивления»: внезапное расширение, разворот потока, совместно с участком радиально окружного течения. Взаимовлияние этих граничных условий предполагает только экспериментальную оценку энергетических потерь в тангенциальном подводящем устройстве через коэффициент потерь местного сопротивления в диапазоне изменения геометрических и режимных параметров.

В результате экспериментальных исследований предложена база данных по коэффициенту потерь тангенциальных подводящих устройств микротурбины в области практического диапазона существования режимных и конструктивных параметров.

Ключевые слова: турбины реактивные, центробежные, коэффициент потерь полной энергии, тангенциальные подводящие устройства, рабочее колесо, окружная работа на турбине, цикл Ренкина, низкокипящее рабочее тело.

Power engineering of the tangential supply device of the microturbine of the thermal control system of a promising spacecraft

Yu. N. Shevchenko, A. A. Kishkin^{*}, A. A. Zuev, A. V. Delkov, D. A. Zhuikov

Reshetnev Siberian State University of Science and Technology
31, Krasnoyarskii rabochii prospekt, Krasnoyarsk, 660037, Russian Federation
^{*}E-mail: spsp99@mail.ru

This paper presents an overview of the current technical problem related to two-phase spacecraft thermal control systems and possible technical applications of thermal energy recovery in the organic Rankine cycle as an integral part of thermal management systems. The design solution involves the integration of a steam microturbine behind an evaporator radiator. The microturbine is a tangential supply device and a radially centripetal impeller of low speed $n_{st} < 40$. In this area, there is no reliable data on the design and energy of both the supply device and the impeller. The energy (loss of enthalpy) of the supply device mainly determines the transport of the swirling flow to the impeller and, as a result, the circumferential operation on the turbine. A prototype of a radial microturbine has been developed and presented in order to evaluate the design of the flow part of both the supply device and the impeller. As a result of the analysis, the main determining hydrodynamic areas necessary for hydrodynamic analysis and mathematical elaboration of the flow calculation algorithm with an assessment of energy losses are identified: the flow of a swirling flow of a radial-annular slit; axial-annular slit and tangential supply device. The first two algorithms assume computational modeling, the model of energy losses in a tangential supply device is not amenable to analytical modeling because it includes a sequence (or compatibility) of flows under boundary conditions defined as "local resistances": the sudden expansion, reversal of the flow, together with a section of radially circumferential flow, the mutual influence of these boundary conditions assumes only an experimental assessment of energy losses in a tangential supply device through the loss coefficient of local resistance in the range of changes in geometric and operating parameters.

As a result of experimental studies, a database has been proposed on the loss coefficient of tangential microturbine supply devices in the field of the practical range of the existence of operating and design parameters.

Keywords: jet turbines, centrifugal turbines, total energy loss coefficient, tangential supply devices, impeller, circumferential turbine operation, Rankine cycle, low-boiling working fluid.

Introduction

Analysis of information on modern foreign developments in the field of using two-phase circuits (TPC) on a spacecraft (SC), which have high energy consumption, shows the technical promise of using them in thermal control systems. Among the spacecraft using phase transition in thermal control systems, NASA's Eureka and Columbus are mentioned, on which full-scale tests of highly efficient two-phase modules were successfully carried out. On the COMET spacecraft (NASA), the thermal regime of individual heat-stressed payload blocks is ensured using thermal control systems (TCS) on capillary pumps. Capillary pumps in the drop-down design of the radiative radiator are also used on the STENTOR spacecraft (NASA) in TCS. Full-scale tests carried out on these spacecraft showed the high efficiency of TCS based on two-phase circuits.

The use of generation using circuits on low-boiling working fluids on ships for long-distance space flights for their energy supply was proposed in the USSR in the seventies of the last century. Unified radioisotope source modules (Pu-238) were used as a heat source for the power steam turbine cycle [1]. The result of the research was an installation with a nominal power of 1.3 kW, a mass of 205 kg and equipped with a refrigerator-emitter with an area of 10.8 m². During bench tests, the mass flow through the circuit reached 0.0107 kg/s. The installation operated for 20 hours. During this time, no significant deviations in parameters were detected.

To solve the problems of thermal regulation of promising large-sized spacecraft and stations with increased power equipment, if it is necessary to reduce the relative mass and size of the spacecraft TCS, the most promising way is to create the basic elements of integrated TCS SC with TPC, as the most effective in comparison with those currently existing in Russia and in foreign practice by means of thermal control. With existing systems, it is necessary to significantly increase the area of external radiator emitters, which leads to an increase in their weight and dimensions. Combining a thermal control system with a steam turbine makes it possible to remove part of the energy through the steam turbine into the power supply system, which reduces the thermal load on the radiator-emitter. The problem of radiator-emitters arises when there are limited possibilities for placing them under the fairing of the launch vehicle at the site of launching the spacecraft into orbit.

Basic technical proposal

The content of the technical solution is determined in accordance with sources [2–4]:

- a direct cycle on low-boiling bodies with generation of mechanical energy. The internal heat source of the spacecraft is used as an energy source, this is the heat generated by operating instruments and installations. In the traditional scheme, this heat is removed into space using radiator refrigerators. The proposed option allows saving energy resources and generating mechanical energy, as well as reducing the area of radiator refrigerators;
- a direct cycle on low-boiling bodies with the generation of mechanical energy using solar heat removed from solar panels as a source. Due to the relatively low equilibrium temperatures of the panels, it has low efficiency, but allows the use of solar radiation in a wider infrared (thermal) range. Installations made using this method are not subject to aging and degradation of characteristics (compared to solar batteries);
- the same as in the previous paragraph, using parabolic-type solar concentrators allows obtaining high temperatures, and therefore high efficiency of the installation. However, in this case it is necessary to solve the problem of high pressure drops of the working fluid in the system.

Microturbine design diagram

In the theory of turbine construction, the relation is mainly used for calculating and designing high-speed turbine stages $n_{st} = 24$ of both axial and radial-centripetal designs [2; 5–9]. This topic is devoted to most of the literature relating to various branches of turbine construction: turbines for large power generation (power plants), turbines for transport devices (aircraft, ground, railway transport, various special-purpose devices, etc.). Most turbines are designed as high-power active-type stages, more than 100 kW. In the field of distributed energy and the practical use of low-grade waste heat, radial-centripetal type turbines with a power of less than 100 kW with a speed coefficient $n_{st} = 60$ are used [4; 6; 10]. The gas dynamics relation is mainly used at supercritical (supersonic) pressure and temperature differences. The topic of structural calculations and optimization of parameters is presented quite comprehensively. For the low speed range $n_{st} < 60$, the topic is not sufficiently covered in terms of engineering calculation applications, which causes obvious difficulties when modeling such objects with a power of less than 100 kW. Today, turbines of various special designs are used to utilize the energy of gas transportation systems and hydrocarbon production systems: including vortex, bladeless and centrifugal, etc. [7].

In our case, turbines with a power of less than 1 kW can be identified (classified) as microturbines of low speed, size and power [11]. The question of optimal design and choice of turbine type remains open due to the low efficiency of low-speed turbomachines, which has similar values for blade-axial and radial microturbines, labyrinth-vortex, disk turbines, centrifugal and centripetal type turbines, etc. It is impossible to give preference to any type at this stage. It is worth noting that for turbines of both active and reactive types, the most important element that forms the circumferential direction of the flow, ensuring the circumferential operation of the impeller, is the nozzle or guide apparatus for high-speed turbines, made in the form of nozzle arrays (in the blade rim). For low-speed and low-flow ma-

chines, one nozzle is made (tangential nozzle channel) [2]. The range of output power according to the customer's technical specifications is from 100 to 1000 W at a subsonic drop working fluid (steam), with a temperature difference of no more than 60 °C with limited speed up to 5000 rpm due to high resource requirements. Given such data, high efficiencies comparable to those of large-scale power turbines should not be expected. The problem of optimal design with the goal of achieving the highest efficiency is relevant. To set the research objectives, a prototype microturbine with a generator with characteristic structural elements based on the centripetal impeller of an expander was designed and manufactured (Fig. 1).

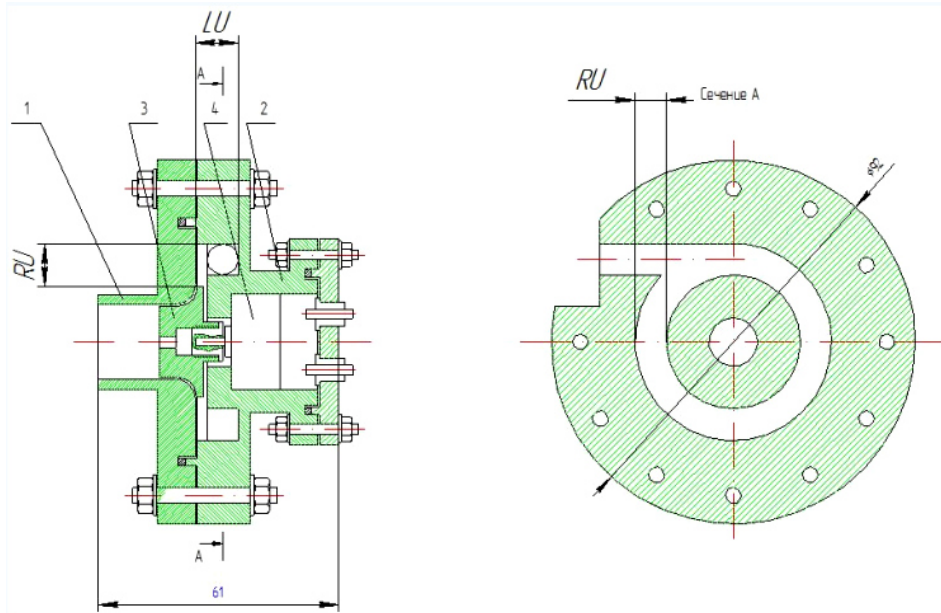


Рис. 1. Прототип микро турбогенератора:
1 – крышка; 2 – корпус микротурбины с тангенциальным подводящим устройством; 3 – рабочее колесо; 4 – генератор

Fig. 1. Prototype of a microturbo generator:
1 – cover; 2 – microturbine housing with tangential supply device;
3 – impeller; 4 – generator

It is clear from the design that the tangential channel is the main element that forms the circumferential flow of the flow. Structurally, the region of radial-circumferential flow RU and axial-circumferential flow LU should be distinguished. General view of the turbogenerator is shown in Fig. 2.

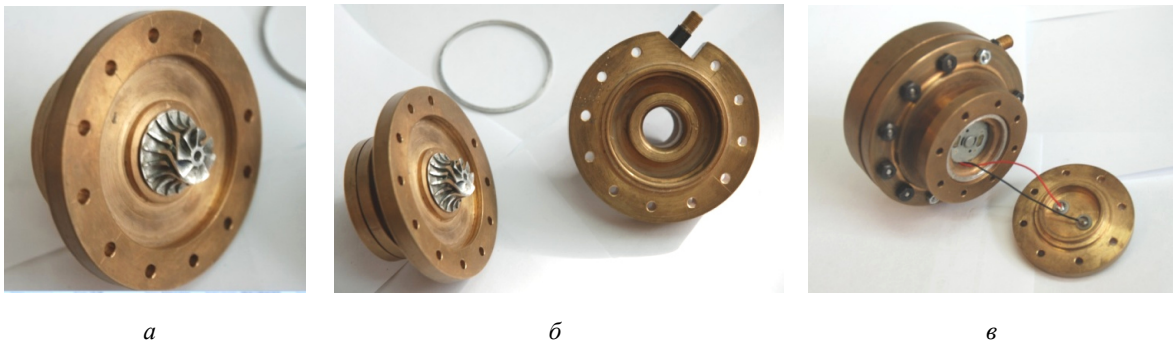


Рис. 2. Вид на рабочее колесо со стороны крышки (а); крышка и корпус генератора (б); вид со стороны крышки генератора (в)

Fig. 2. View of the impeller from the cover side (a); cover and housing of the generator (b); view from the side of the generator cover (c)

Purpose and statement of the research problem

The current designs of TCS of autonomous spacecraft with a long active life (up to 15 years) use almost the entire range of known design solutions: natural thermal conductivity from the source to the radiator-emitter into black space; complex design of the transport heat pipe system; liquid-circuit heat transfer from the southern to the northern panel, TPC with a dynamic (pump) supply system in the circuit to the circuit heat pipe. The specified list in sequence ensures an increase in the mass-energy characteristics of the TCS system [12]. It should be noted that the dimensions of the northern and southern panels are determined by the area of the evaporator and condenser TCS integrated into the honeycomb panels, and mainly determine the dimensions and power circuit of the spacecraft as a whole. The next logical step is the recovery of electrical energy in a two-phase TCS system based on the organic Rankine cycle in order to reduce the thermal load on the emitter capacitor. The most important component of such a system is a turbo drive, consisting of a supply device that provides a field of velocities and pressures at the inlet into the subsequent turbine impeller. Low-speed turbines with low-flow partial supply are characterized by significant asymmetry in the fields of thermodynamic parameters, leading to significant deviations in the calculation results using the methods of full-size units. In accordance with the above, following the set goal of increasing the mass-energy characteristics of two-phase TCS through the use of a turbogenerator in the Rankine cycle, it is necessary to solve the following problems:

- develop and manufacture a set of standard sizes of supply devices in order to obtain energy characteristics in the range of changes in design and operating parameters;
- to conduct experimental studies of the energy characteristics of supply devices with the creation of a database on the main design and operating parameters.

Methodology for conducting energy and partial balance tests of microturbines

Energy tests are carried out with elements of balance tests, possible on the material part of the physical model with the additional installation of measuring (stations) posts: p^* is total pressure; p is static pressure; T_{meas} is a measured equilibrium temperature.

The location of posts (measuring stations), for the purpose of correcting the calculation algorithm, completely coincides with the accepted calculation scheme (Fig. 3).

The sequence of measurement posts corresponds to:

- measurement post in front of the entrance to the channel inlet $p_2^*, p_{\text{ent}}^*, T_{\text{ent}}^*, T_{\text{ent}}$;
- in the channel of the supply device $p_0, p_0^*, T_{0\text{meas}}$;
- at the outlet of the channel supply device, at the inlet to the impeller p_1, p_{1u}^* , на выходе из канального подводящего устройства, на входе в рабочее колесо $p_1, p_{1u}^*, T_{1\text{meas}}$,

where p_{1u}^* is measured in the circumferential direction;

- at the outlet of the impeller at radius $R_2, p_2, p_{2u}^*, T_{1\text{meas}}$.

Since it is technically difficult to place a total pressure receiver at radius R_1 , purging of channel supply devices is carried out in a special device, without an impeller, at the radius of the entrance to the impeller. If necessary, these tests are coordinated by p_1 - static pressure during energy tests.

Methodology for processing results in the post /ent – 0/ is considered below.

$p_{\text{ent}}^*, T_{\text{ent}}^*, p_0, p_0^*, T_{0\text{meas}}, M_0, T_0, \tau_{f0}, C_0$ are measured.

Additionally, it calculates mass flow in two ways to eliminate errors.

$$\square \quad m = \rho_0 \cdot C_0 \cdot F_0 = \rho_0 \cdot F_0 \cdot m \cdot q_{f0}, \quad (1)$$

where

$$m = \sqrt{k \left(\frac{2}{k+1} \right)^{\frac{k+1}{k-1}} \cdot \frac{1}{R}}, \quad (2)$$

$$q_{f0} = \left(\frac{k+1}{2} \right)^{\frac{k+1}{2(k-1)}} \cdot \frac{M_0}{\left(1 + \frac{k-1}{2} \cdot M_0^2 \right)^{\frac{k+1}{2(k-1)}}}. \quad (3)$$

$F_0 = h_0 \cdot b_0$ is a flow area of the supply channel.

The loss coefficient ζ_{ent} is calculated:

$$\frac{2}{C_0} \cdot \frac{k}{(k-1)} \left(\frac{p_{ent}^*}{\rho_{ent}} - \frac{p_0^*}{\rho_0} \right) = \zeta_{ent}. \quad (4)$$

Methodology for processing results in the area $/0 - 1/$ are considered.

p_{1u}^*, p_1, T_{1meas} are measured.

p_0, p_0^*, T_{0meas} are known.

They are calculated using expressions for the circumferential component C_{1u} :

$$M_{1u}, T_{1u}, \tau_{f1}, C_{1u}, p_u, T_{1u}^*. \quad (5)$$

The parameters are calculated based on the circumferential component C_{1u} , correction is necessary:

$$C_1 = \sqrt{C_{1u}^2 + C_{1R}^2}. \quad (6)$$

where C_{1R} is the radial component of the absolute velocity at the inlet; it is determined in a first approximation $p_1 = p_{1u}$ and

$$C_{1R} = \frac{\dot{m}}{\rho_1 \cdot F_2} = \frac{\dot{m}}{\rho_1 \cdot 2\pi R_1 \cdot b_1}, \quad (7)$$

where \dot{m} (1).

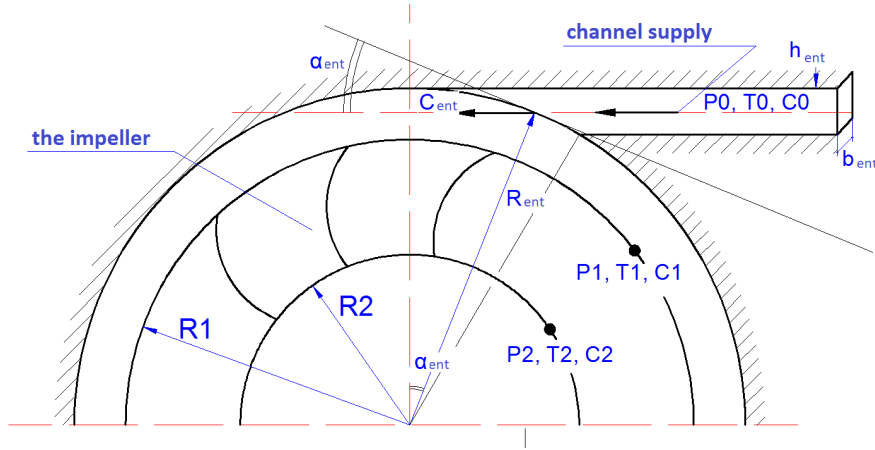


Рис. 3. Расчетная схема радиальной ступени

Fig. 3. Design scheme of the radial stage

Total pressure is corrected:

$$p_1^* = p_1 + \frac{C_1^2}{2} \cdot \frac{k-1}{k}. \quad (8)$$

And the run is performed while:

$$\frac{C_{li+1} - C_{li}}{C_{li+1}} \leq 0.01.$$

With C_1 , C_{1u} , C_{1R} known, the absolute velocity angle is calculated:

$$\alpha_1 = \arctg \frac{C_{1R}}{C_{1u}}. \quad (9)$$

There is a relative velocity angle:

$$\beta_1 = \arctg \frac{C_{1R}}{C_{1u} - U_1} = \arctg \frac{C_{1R}}{(C_{1u} - \omega_1 \cdot R_1)}, \quad (10)$$

$$W_1 = \frac{|C_{1u} - U_1|}{\cos \beta_{1\pi}}.$$

There is an attack angle:

$$i = \beta_{1\pi} - \beta_1, \quad (11)$$

where $\beta_{1\pi}$ is a design parameter.

Nozzle (feeder) loss coefficient is the following:

$$\zeta_{C_0} = \left(\frac{p_0^*}{\rho_0} - \frac{p_1^*}{\rho_1} \right) \cdot \frac{2}{C_0^2} \cdot \frac{k}{(k-1)}. \quad (12)$$

Description and design features of the studied channel supply lines devices

Experimental purging of channel supply devices was carried out in a special device that simulates a power plant and allows measurements to be taken at six measuring stations, according to the diagram (Fig. 4).

Here are measuring post at the input p_{ent} , T_{ent} , p_{bx} , T_{bx} , measuring post in the channel of the supply device p_0 , T_0 and four measuring posts on the radius of the impeller p_1T_1 , p_2T_2 , p_3T_3 , p_4T_4 . No measurements were taken at the p_2T_2 post; the post is a backup one. At each post, total pressure (p^*) was measured with a total pressure receiver and static pressure (p_{st}) with a static pressure receiver, and the equilibrium measured temperature (t) was measured with a thermocouple.

The experimental setup with placed total and static pressure receivers is shown in Fig. 5.

For geometric parameters, the following definitions and design relationships are used:

– l_{ent} is an angular momentum arm, where:

$$l_{ent} = R_{ent} - h / 2;$$

– $d_{g,eq}$ is the equivalent throat diameter, where

$$d_{g,eq} = \sqrt{\frac{4 \cdot b \cdot h}{\pi}};$$

– ε is a degree of partiality, where

$$\varepsilon = \frac{\alpha_{ent}}{2\pi}, \quad \alpha_{ent} = \arccos \frac{R_{ent} - h}{R_{ent}};$$

Re_0 is the Reynolds number at speed C_0 , where

$$Re_0 = \frac{C_0 \cdot d_{g,eq}}{\nu};$$

Re_ω is the Reynolds number along the peripheral speed, where

$$\text{Re}_\omega = \frac{C_0 l_{ent}}{v} = \frac{\omega \cdot l_{ent}^2}{v};$$

– l_{ent}/R_{1k} is the relative angular momentum arm, where $R_{1k} = 24$ mm is the radius of the entrance to the microturbine impeller.

A spiral supply device is formed by combining two profiling radii R_1 and R_2 with a displacement of the profiling centers by an amount Δ .

Measured parameters of the microturbine spiral feed device are the following:

$b = 3.5$ mm is the channel width;

D is an outer maximum diameter;

δ is the distance from D to the upper (closest to D) surface of the channel h ;

L_1 is the maximum distance along the line of diameter D ;

h is the width of the input channel;

R_1 is the larger profiling radius;

R_2 is the smaller profiling radius;

Δ is the displacement of profiling centers;

ε is the degree of partiality;

l_{ent} is the arm of the input channel along the midline;

h/R_{1k} is the relative width of the input channel;

l_{ent}/R_{1k} is the relative width of the input channel.

$$d_{g.eq} = \sqrt{\frac{4 \cdot b \cdot h}{\pi}}.$$

Here are expressions for calculating a spiral drive device based on measurement results:

$$L_1 = R_1 + R_2 + 2\Delta;$$

$$\Delta = 0.5h + \delta + 0.5L_1 \cdot 0.5D,$$

$$R_1 = D - 2\delta - 0.5h - 0.5L_1,$$

$$R_2 = 0.5(L_1 - h),$$

$$l_{BX} = 0.5D - \delta - 0.5h,$$

$$\alpha_{ent} = \arccos \frac{l_{ent} - 0.5h}{l_{ent} + 0.5h},$$

$$\varepsilon = \frac{\alpha_{ent}}{2\pi}.$$

Here are expressions for calculating a ring drive device:

$$R_1 = \frac{L_1}{2},$$

$$l_{ent} = 0.5L_1 - 0.5h,$$

or

$$l_{ent} = R_1 - \frac{h}{2}.$$

The following designations for collectors are accepted: C is spiral, the first digit in the designation: height h in mm. The second digit in the designation: l_{ent} is an arm of the moment of momentum in mm (rounded), for example: C6–39 is spiral $h = 6$ mm, $l_{ent} \approx 39$ mm; K6–32 is ring $h = 6$ mm, $l_{ent} \approx 32$ mm.

According to the designations, the quantitative values of the parameters of 19 spiral and 13 ring supply devices are presented in Table. 1.

Table 1

Range of design parameters for spiral and ring feed devices

Designation	h (mm)	L_{ent} (mm)	$D_{g. eq}$ (mm)	L_{ent}/R_{lk}	h/R_{lk}
C2...6-28...39	2-6	28-38.9	3-5.2	1.16-1.62	0.083-0.25
K2...6-25...32	2-6	25-32	3-5.2	1.04-1.33	0.083-0.25

You can see the range of change of geometric parameters in dimensionless (relative) form (22 structural assemblies):

$Re_0 = 10000-60000 = 1 - 6 \cdot 10^4$ is the Reynolds number for speed C_0 ;

$L_{ent}/R_{lk} = 0.97-1.62$ is a relative input arm;

$h/R_{lk} = 0.083-0.25$ is the relative width of the input channel;

$b = 3.5$ mm is the channel width;

$R_{lk} = 24$ mm is the radius of entry into the microturbine impeller.

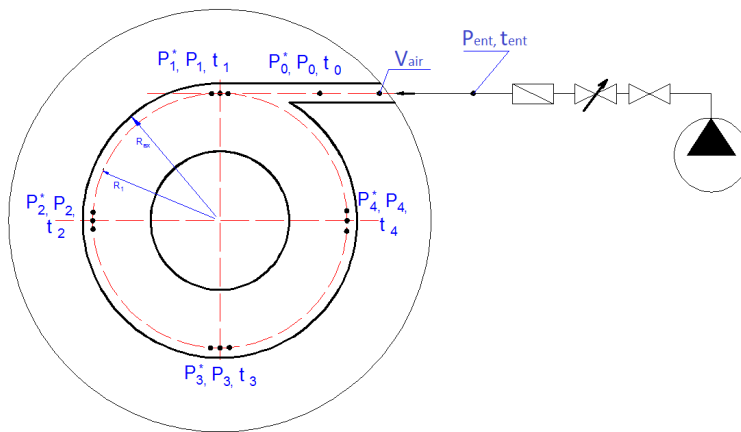


Рис. 4. Схема расположения датчиков в испытательной системе

Fig. 4. The layout of the sensors in the test system

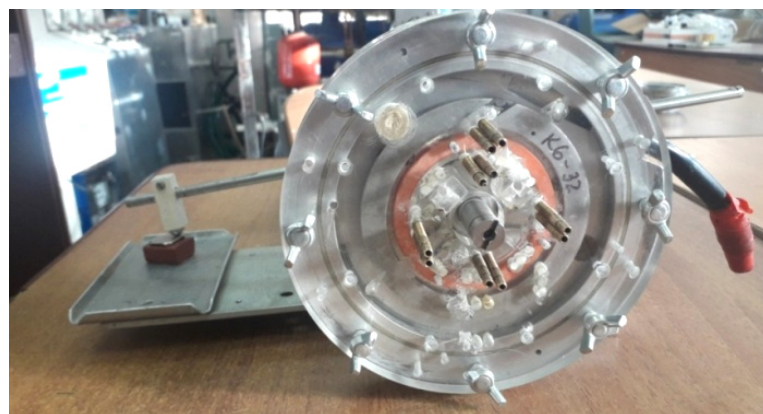


Рис. 5. Экспериментальная установка с приемниками полного и статического давления

Fig. 5. Experimental installation with full and static pressure receivers

Methodology for processing experimental tests of tangential supply of a subsonic centripetal turbine

To develop a mathematical model and algorithm for calculating a centripetal microturbine used to utilize the thermal power of a spacecraft, it is necessary to estimate the circumferential component of the absolute speed at the radius of the entrance to the turbine impeller (TI). Theoretical analysis of total flow losses as a superposition of sudden expansion with subsequent vortex flow to the impeller represents a theoretically uncertain problem. For a preliminary assessment and formation of a database of losses in this section, it is necessary to use data from experimental blowdowns with registration of energy and speed parameters of the flow in the section: 0 – parameters in the input channel of the device; 1 – parameters on the inlet diameter in the inlet channel of the device. To process experimental data, in addition to the energy loss coefficient ζ_{01} , it is convenient to use the coefficient of the circumferential velocity component φ_u [13–15].

Let us justify some considerations that determine the content of the coefficient of the circumferential velocity component and determine the mass flow rate in the supply channel:

$$\dot{m} = \rho \dot{V} = C_0 \cdot h_0 \cdot b_0, \quad (13)$$

where ρ is density; C_0 is the flow rate in the channel; h_0 is the channel height; b_0 is the width.

Let us assume that C_0 is const along the height h_0 , the angular momentum arm along h_0 changes from l_1 до l_2 , and then the angular momentum in the input section will be written as an integral:

$$M_0 = \int_{l_1}^{l_2} \rho \cdot C_0^2 \cdot l \cdot b_0 \cdot dl = \rho \cdot C_0 \cdot h_0 \cdot b_0 \cdot C_0 \frac{l^2}{2} \Big|_{l_1}^{l_2}. \quad (14)$$

Let us substitute the limits of integration $l_2 R_0$; $l_1 = R_0 - h_0$ and take into account (13):

$$M_0 = \dot{m} \cdot C_0 \cdot \frac{1}{2} (l_2^2 - l_1^2),$$

$$M_0 = \frac{1}{2} \dot{m} \cdot C_0 (2R_0 h_0 - h_0^2) = \dot{m} \cdot C_0 h_0 \left(R_0 - \frac{h_0}{2} \right). \quad (15)$$

Theoretical angular momentum at the current radius R is the following:

$$M_T = \dot{m} \cdot U_T \cdot R, \quad (16)$$

where \dot{m} is the mass flow determined by the expression:

$$\dot{m} = 2\pi R \cdot b \cdot C_R \cdot \rho. \quad (17)$$

For the ideal case, when there is no friction torque, the moments M_0 and M are equal:

$$M_0 = M_T,$$

Substituting expressions for moments (16), we obtain:

$$\dot{m} \cdot C_0 \cdot h_0 \left(R_0 - \frac{h_0}{2} \right) = \dot{m} \cdot U_T \cdot R, \quad (18)$$

Let's continue the transformation, expressing the values of the circumferential component at the current radius through the parameters in the input channel:

$$U_T = \frac{C_0 h_0}{R} \left(R_0 - \frac{1}{2} h_0 \right), \quad (19)$$

or taking into account

$$R_0 = l_{ent} + \frac{h_0}{2},$$

$$U_T = \frac{C_0 h_0}{R} \cdot l_{ent}, \quad (20)$$

For the radius of entry into the impeller R_1 in the absence of losses

$$U_{1T} = \frac{C_0 h_0}{R_1} \cdot l_{ent}, \quad (21)$$

The coefficient of the circumferential velocity component is determined

$$\varphi_u = \frac{U_{1\partial}}{U_{1T}}, \quad (22)$$

where $U_{1\partial}$ is the actual (measured) value; U_{1T} is the maximum theoretically possible.

The actual value of the peripheral speed is calculated as the average of the results of measurements of total and static pressure and temperature along the periphery of the microturbine impeller at 4 points of the circle R_1 (Fig. 4).

A general view of the assembly is shown in Fig. 6, where the connections to the thermistors are shown, and the pressure receivers are not connected to the measuring tubes of the pressure sensors.

For a preliminary assessment of the peripheral speed at the entrance to the microturbine rotor of the LV, it is necessary to use the energy equations along the periphery of the microturbine:

$$\frac{k}{k-1} \cdot \frac{p_0}{\rho_0} + \frac{C_0^2}{2} = \frac{k}{k-1} \cdot \frac{p_1}{\rho_1} + \frac{C_1^2}{2} + \zeta_c \cdot \frac{C_0^2}{2}, \quad (23)$$

where ζ_c is the total pressure loss coefficient in the nozzle; absolute speed at the entrance to LV:

$$C_1^2 = U_1^2 + C_{R1}^2, \quad (24)$$

the consumption component is determined only by calculation:

$$C_{R1} = \frac{\dot{m}}{\rho_1 F_1}, \quad (25)$$

where \dot{m} is the mass flow of the working fluid; ρ_1 is the density at the entrance to the LV; F_1 is the flow section area to the LV.

The speed coefficient is a parameter calculated directly from measurement results without additional assumptions. According to the results of the experiment in the range of changes in the geometric and operating parameters of the microturbine supply device (h_0 – channel height; l_{ent} – average arm of the angular momentum; R_1 – radius of the entrance to the impeller; Re – Reynolds number at the entrance) the possibility of forming a database for φ_u is realized for the purpose of using it in mathematical modeling and design of a microturbine.

The use of databases on the circumferential velocity component coefficient φ_u (22) and the total pressure loss coefficient ζ_c (23) makes it possible to unambiguously determine the total pressure at the inlet to the microturbine valve during mathematical modeling and design, and also carry out optimization in the range of changes in the operating and geometric parameters of the microturbine.

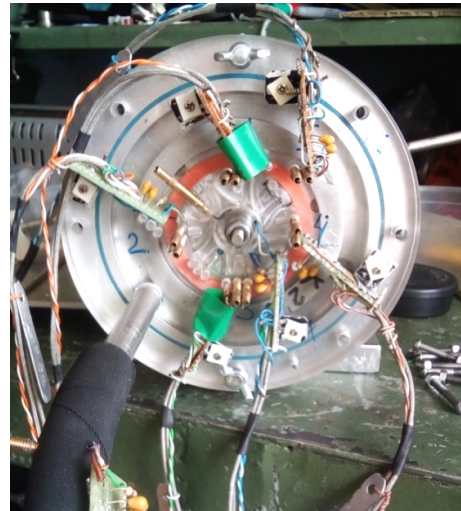


Рис. 6. Общий вид сборки

Fig. 6. General view of the assembly

The algorithm for processing experimental data from tests of tangential, spiral and annular inlets is implemented in the form of a software algorithm that allows, based on measurements in 0 (channel inlet) and 1 section (along the periphery of the impeller), values of pressure, temperature and design speeds, to determine the energy parameters of the inlet device: ζ_c as the loss coefficient (12) and φ_u as the speed coefficient (21).

According to the design diagrams of the material part for spiral and ring supply devices, experimental measurements of the loss coefficient ζ_{c0} and φ_u were carried out in the range of changes in the geometry of the supply devices (Tables 1, 2) and the operating parameter Re_0 , calculated from the value of the speed C_0 (U_0) in the tangential supply. The data is presented in the form of a database in Tables 2, 3. In general, the database is a tabular function of the loss coefficient $\zeta_{c0} = (L_{ent} / R_{lk}, h / R_{lk}, Re_0)$; a tabular function of the speed coefficient $\varphi_u = (L_{ent} / R_{lk}, h / R_{lk}, Re_0)$; from three variables:

L_{ent}/R_{lk} is a relative input arm;

h/R_{lk} is a relative width of the input channel;

Re_0 is the Reynolds number for the velocity $C_0(U_0)$ in the tangential channel.

According to the tabular data, visualization of the level surface, the function is quite monotonic, does not have sharp extrema, and is quite easily approximated even by linear splines (Fig. 7). The value of the function is 2–3 times higher than the loss coefficient due to sudden expansion. Obviously, there must be an additional element in the structure of energy losses. As such an element, we should consider the loss of flow energy when the flow flows from radius R_0 to radius R_{lk} , which follows from the structural geometry of the supply device. To estimate the loss coefficient in the radially circumferential section of the flow, we will use a numerical estimate based on test data of the K2-25 annular supply device.

We use the values of $R_0 = l_{ent} + h / 2 = 0.026$ m; $\Delta R = R_0 - R_k = 0.002$ m; $\delta_\alpha^{**} = 0.00017$ m; $C_{u0} = U_0 \cdot R_0 = 2.314$ [m²/c] as the initial data for the calculation. Loss factors are calculated using the expression derived from the energy equation:

$$\frac{k}{k-1} \cdot \frac{p_0}{\rho_0} + \frac{U_0^2}{2} = \frac{k}{k-1} \cdot \frac{p_1}{\rho_1} + \frac{U_1^2}{2} + \zeta_{rad.uch.} \cdot \frac{U_0^2}{2},$$

from which $\zeta_{rad.uch.}$:

$$\zeta_{rad.uch.} = \frac{2}{U_0^2} \left(\frac{k}{k-1} \cdot \frac{1}{\rho} (p_0 - p_k) + \frac{U_0^2 - U_k^2}{2} \right). \quad (26)$$

It should be noted that the loss coefficient in the radial flow section is formed due to a drop in static pressure and the circumferential velocity component. In one dimension potential flow, the change in total and static pressures coincides, the speed does not change. The calculation results are presented in table. 4 [16–17]. It is clear from the results that the loss coefficient changes almost twice as Reynolds changes and is close to one. The loss coefficient is formed from two approximately identical terms: losses of static pressure, losses of peripheral speed.

Taking into account the data of the coefficient for sudden expansion and the loss coefficient, approximately 1/3 of the total loss coefficient remains in the radial section, i.e., a value approximately equal to unity. As a hypothesis, it is proposed to estimate this value by the loss coefficient for a flow turn of 90° using the Weisbach formula [14]:

$$\zeta_M = 0.95 \sin^2 \left(\frac{\delta}{2} \right) + 2.05 \sin^4 \left(\frac{\delta}{2} \right) = 0.986,$$

where $\delta = 90^\circ$ is a rotation angle, taking into account the correction loss coefficient for rotation $\zeta_{pov} = C_1 \cdot A \cdot \zeta_M$; $C_1 = 1$ for symmetrical flow; $A = 0.95 + 33.5 / \delta = 1.32$; then the reversal coefficient

is $\zeta_{90^\circ} = 1.3$. It should be noted that the proposed energy balancing of losses for sudden expansion, radial section and flow reversal by 90° gives the value placed in the database for the loss coefficient ζ_{c0} in the supply device (Tables 2, 3).

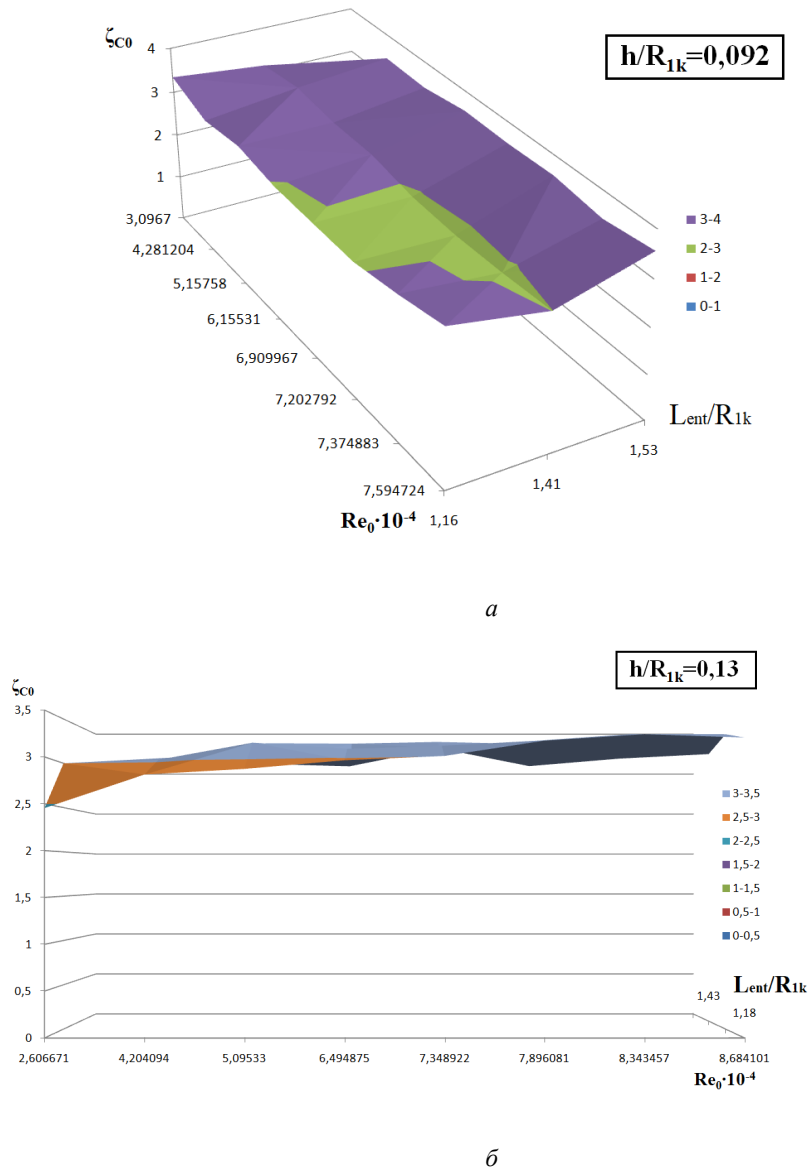


Рис. 7. Поверхности уровней функции (базы данных) $\zeta_{c0} = (L_{ent} / R_{lk}, h / R_{lk}, Re_0)$:
 а – относительная ширина входного канала $h / R_{lk} = 0.092$; б – $h / R_{lk} = 0.013$

Fig. 7. Surfaces of function levels (databases) $\zeta_{c0} = (L_{ent} / R_{lk}, h / R_{lk}, Re_0)$:
 а – relative width of the input channel $h / R_{lk} = 0.092$; б – $h / R_{lk} = 0.013$

Table 2

Loss coefficients ζ_{C0} and speed φ_u for a ring supply device

K2-25					K6-32				
ζ_{C0}	L_{ent}/R_{1k}	h/R_{1k}	Re_0	φ_u	ζ_{C0}	L_{ent}/R_{1k}	h/R_{1k}	Re_0	φ_u
3.0209067	1.04	0.083	17520.65	0.2889737	2.6914906	1.33	0.25	28199.46	0.350395
2.81332385	1.04	0.083	21327.45	0.4220766	1.3009716	1.33	0.25	24833.99	0.5772179
2.7729739	1.04	0.083	26275.56	0.4445341	1.2320646	1.33	0.25	31322.3	0.5997001
3.1156121	1.04	0.083	29045.19	0.3552896	1.732688	1.33	0.25	39639.36	0.5403541
2.8642894	1.04	0.083	30264.05	0.4435942	2.0409651	1.33	0.25	44025.96	0.5012578
2.880883	1.04	0.083	32048.86	0.4319966	1.7411898	1.33	0.25	47618.09	0.5481886
2.7712986	1.04	0.083	32068.46	0.4661496	1.8086491	1.33	0.25	50644.91	0.541099
2.8155358	1.04	0.083	30754.69	0.4596947	1.7884947	1.33	0.25	50892.56	0.5436699

Table 3

Loss coefficients ζ_{C0} and speed φ_u for a spiral feed device

C2-28					C6-39				
ζ_{C0}	L_{ent}/R_{1k}	h/R_{1k}	Re_0	φ_u	ζ_{C0}	L_{ent}/R_{1k}	h/R_{1k}	Re_0	φ_u
3.3439123	1.16	0.083	30933.17	0.2453211	1.7325754	1.62	0.25	19870.44	0.4304552
3.01471724	1.16	0.083	38247.2	0.3147172	2.6571707	1.62	0.25	30967.94	0.3141631
3.1387546	1.16	0.083	45548.23	0.3981814	1.9631256	1.62	0.25	32378.77	0.4201886
2.98048791	1.16	0.083	55432.55	0.3672183	2.1385318	1.62	0.25	40561.44	0.4038012
2.9605327	1.16	0.083	60051.83	0.3609476	2.0742571	1.62	0.25	44835.47	0.4082927
2.9455596	1.16	0.083	64664.08	0.3731699	1.8497709	1.62	0.25	52284.86	0.4391877
3.12578929	1.16	0.083	67022.12	0.3387341	1.801266	1.62	0.25	54236.36	0.445411
3.3556589	1.16	0.083	69246.83	0.2580974	1.6874583	1.62	0.25	58712.84	0.4565281

Table 4

Results of calculations of loss coefficients in the radial section of the flow

N_0	$C_{0f}(U_0)$ [m/s]	p_0^* [Pa]	p_0 [Pa]	τ_{0u} [Nwm ²]]	dC_u/dR [m/s]	C_{u0} [m ² /s]]	ΔC_{u0} [m ² /s]	C_{uk} [m ² /s]	U_k [m/s]	Δp [Pa]	p_k [Pa]	$\frac{2k}{(k-1)\rho} \cdot \frac{p_0 - p_k}{U_0^2}$	$\left(1 - \frac{U_k}{U_0}\right)^2$	$\zeta_{rad.uch.}$	Re_0
1	89	103750	98955	31.4	408.2	2.314	0.816	1.5	62.4	662	98923	0.487	0.508	0.995	17500
2	107	111260	103710	43.32	458.4	2.782	0.916	1.87	77.8	961	102749	0.518	0.471	0.983	21300
3	133	123277	110844	63.4	544.3	3.458	1.09	2.37	98.7	1493	109351	0.492	0.449	0.941	26286
4	147	139803	122733	75.5	582.2	3.828	1.16	2.662	111	1828	120905	0.493	0.43	0.923	29045
5	153	157831	13700	81.0	594.4	3.98	1.19	2.8	116	1982	135018	0.4936	0.425	0.919	30264
6	162	174356	148890	89.23	610.5	4.2	1.221	2.98	124	2216	146674	0.494	0.412	0.906	32048
7	162	193866	165535	89.4	598.2	4.21	1.196	2.014	125.6	2223	163312	0.4944	0.398	0.8924	32068

Conclusion

Based on the research results, it is clear that the tangential supply device of a radial microturbine topologically represents boundary flow conditions that consistently combine hydraulic losses of local resistance: sudden expansion, flow reversal by 90° , flow in a radially swirled section in front of the impeller. Formally, hydraulically, local losses are summed up through hydraulic straight sections. In our case, local resistance losses are combined and mutually influence each other, which excludes their summation in the general case [14]. Therefore, from the point of view of the adequacy of the results, it is preferable to use the loss coefficient database in the supply device. Addition of losses is possible only as an approximate estimate.

1. Experimental results on the loss coefficient $\zeta_{c0} = (L_{ent} / R_{lk}; h / R_{lk}; Re_0)$ and for annular and spiral tangential supply devices are presented in the form of a database. In general, the database is a table function of three variables:

L_{ent}/R_{lk} is a relative input arm;

h/R_{lk} is a relative width of the input channel;

Re_0 is the Reynolds number for the velocity $C_0(U_0)$ in the tangential channel.

2. The loss coefficient function is quite monotonic and does not have bright extrema; the value of the function is approximately three times higher than the value for a sudden expansion of the flow, which suggests its additive structure.

3. Based on the results of a comparative energy analysis, in a first approximation, the following structure of energy losses in the tangential supply device of a microturbine is proposed, which is practically consistent with the value of experimental losses: $\zeta_{c0} = \zeta_{vn.rash.} + \zeta_{90^\circ} + \zeta_{rad.uch.}$, where $\zeta_{vn.rash.}$ is losses due to sudden expansion; ζ_{90° is losses due to flow reversal by 90° ; $\zeta_{rad.uch.}$ is friction losses on the radial section of the channel.

4. A similar database was obtained for the speed coefficient φ_u .

Библиографические ссылки

1. Органический цикл Ренкина в автономной теплоэнергетической системе : монография / А. А. Кишкин, О. В. Шилкин, А. В. Делков и др. ; СибГУ им. М. Ф. Решетнева. Красноярск, 2019. 234 с.
2. Разработка установок-утилизаторов низкопотенциального тепла на основе органического цикла Ренкина / А. А. Кишкин, Д. В. Черненко, А. А. Ходенков и др. // Альтернативная энергетика и экология. 2014. № 3 (4). С. 35–36.
3. Расчет и анализ тепловых технических систем, работающих по замкнутому циклу / А. А. Кишкин, Е. В. Черненко, Д. В. Черненко и др. // Materiály VIII mezinárodní vědecko – praktická conference “Dny vědy – 2012”. Díl 91. Technické vědy: Praha. Publishing House Education and Science s.r.o, 2012.
4. Боровский Б. И. Энергетические параметры и характеристики высокооборотных лопастных насосов. М. : Машиностроение, 1989. 184 с.
5. Теория пространственного пограничного слоя в гидродинамике турбомашин : монография / А. А. Кишкин, В. П. Назаров, Д. А. Жуйков, Д. В. Черненко ; Сиб. гос. аэрокосмич. ун-т. Красноярск, 2013. 250 с.
6. Кишкин А. А., Зуев А. А., Делков А. В. Трехмерный температурный пограничный слой в теории конвективного теплообмена : монография / Сиб. гос. аэрокосмич. ун-т. Красноярск, 2015. 282 с.
7. Смирнов М. В. Безлопаточные центробежные ступени для турбодетандоров малой мощности : дис. ... канд. техн. наук. СПб. 2019. 154 с.
8. Теплосиловые системы: Оптимизационные исследования / А. М. Клер, Н. П. Деканова, Э. А. Тюрина и др. Новосибирск : Наука, 2005. 236 с.

9. Краев М. В., Лукин В. А., Овсянников Б. В. Малорасходные насосы авиационных и космических систем. М. : Машиностроение, 1985. 128 с.
10. Краев М. В., Кишкин А. А., Сизых Д. Н. Гидродинамика малорасходных насосных агрегатов. Красноярск : САА, 1988. 157 с.
11. Прототипирование микротурбогенератора и постановка задачи исследования / Ю. Н. Шевченко, О. В. Шилкин, А. А. Кишкин и др. // Испытания, диагностика, надежность. Теория и практика : сб. тр. Всеросс. науч.-практ. конф. Красноярск, 2023. С. 17–21.
12. Моделирование и конструирование двухфазных систем термо- регулирования космических аппаратов : монография / О. В. Шилкин, А. А. Кишкин, А. В. Делков, и др. ; СибГУ им. М. Ф. Решетнева. Красноярск, 2022. 192 с.
13. Коэффициент скорости тангенциального подвода дозвуковой центростремительной турбины / Ю. Н. Шевченко, А. А. Кишкин, А. В. Делков, М. У. Абдуллаев // Омский науч. вестник. Серия: Авиационно-ракетное и энергетическое машиностроение. 2022. Т. 6, № 2. С. 78–84.
14. Идельчик И. Е. Справочник по гидравлическим сопротивлениям / под ред. М. О. Штейнберга. М. : Машиностроение, 1992. 672 с.
15. Kishkin A. A. , Shevchenko Yu. N., Delkov A. V. Analysis of the key design features of low-power turbines for electricity generation // IOP Conference Series: Materials Science and Engineering. 2020. Vol. 919. DOI: 10.1088/1757-899X/919/6/062030.
16. Energy equations for the temperature three-dimensional boundary layer for the flow within boundary conditions of turbo machinery / A. A. Zuev, A. A. Kishkin, D. A. Zhuikov et al. // IOP Conference Series: Materials Science and Engineering. 2019. Vol. 537. P. 22008. Doi:10.1088/1757-899X/537/2/022008.
17. Tn. Karman. Uber laminare und turbulente Reibung // ZAAM. 1921. No. 1. P. 233–252.

References

1. Kishkin A. A., Shilkin O. V., Delkov A. V. et al. *Organicheskiy tsikl Renkina v avtonomnoy teploenergeticheskoy sisteme*. [The organic Rankine cycle in an autonomous thermal power system]. Krasnoyarsk, 2019, 234 p.
2. Kishkin A. A., Chernenko D. V., Khodenkov A. A. et al. [Development of low-potential heat recovery plants based on the organic Rankine cycle]. *Al'ternativnaya energetika i ekologiya*. 2014, No. 3 (4), P. 35–36 (In Russ.).
3. Kishkin A. A. Chernenko E. V., Chernenko D. V. et al. Calculation and analysis of thermal engineering systems operating in a closed cycle. *Materiály VIII mezinárodní vědecko – praktická conference Dny vědy – 2012. Díl 91. Technické vědy: Praha. Publishing House Education and Science s.r.o*, 2012.
4. Borovsky B. I. *Energeticheskie pararmetry i kharakteristiki vysokooborotnykh lopastnykh nasosov*. [Energy parameters and characteristics of high-speed vane pumps]. Moscow, Mashinostroenie Publ., 1989, 184 p.
5. Kishkin A. A., Nazarov V. P., Zhuykov D. A., Chernenko D. V. *Teoriya prostranstvennogo pogranichnogo sloya v gidrodinamike turbomashin* [The theory of the spatial boundary layer in the hydrodynamics of turbomachines]. Krasnoyarsk, 2013, 250 p.
6. Kishkin A. A., Zuev A. A., Delkov A. V. *Trekhmernyy temperaturnyy pogranichnyy sloy v teorii konvektivnogo teploobmena* [Temperature boundary layer in the theory of convective heat transfer]. Krasnoyarsk, 2015, 282 p.
7. Smirnov M. V. *Bezlopatochnye tsentrobezhnnye stupeni dlya turbodetandorov maloy moshchnosti. Dis. kand.* [Bladeless centrifugal stages for low-power turbodetandors. Dis. Cand.]. St. Petersburg. 2019, 154 p.
8. Kler A. M., Dekanova N. P., Tyurina E. A. et al. *Teplosilovye sistemy: Optimizatsionnye issledovaniya* [Thermal power systems: Optimization studies]. Novosibirsk, Nauka Publ., 2005, 236 p.
9. Kraev M. V., Lukin V. A., Ovsyannikov B. V. *Maloraskhodnye nasosy aviatsionnykh i kosmicheskikh sistem*. [Low-flow pumps for aviation and space systems]. Moscow, Mashinostroenie Publ., 1985, 128 p.
10. Kraev M. V., Kishkin A. A., Sizykh D. N. *Gidrodinamika maloraskhodnykh nasosnykh agregatov* [Hydrodynamics of low-flow pumping units]. Krasnoyarsk, 198, 157 p.

11. Shevchenko Yu. N., Shilkin O. V., Kishkin A. A. et al. [Prototyping of a microturbogenerator and setting the research task]. *V sbornike: materialov Vserossiyskoy nauchno-prakticheskoy konferentsii "Ispytaniya, diagnostika, nadezhnost'. Teoriya i praktika"* [In the collection: materials of the All-Russian scientific and practical conference "Tests, Diagnostics, reliability. Theory and practice"]. Krasnoyarsk, 2023, P. 17–21 (In Russ.).
12. Shilkin O. V., Kishkin A. A., Delkov A. V. et al. *Modelirovanie i konstruirovaniye dvukhfaznykh sistem termo- regulirovaniya kosmicheskikh apparatov* [Modeling and design of two-phase thermal control systems for spacecraft]. Krasnoyarsk, 2022, 192 p.
13. Shevchenko Yu. N., Kishkin A. A., Delkov A. V., Abdullaev M. U. [The speed coefficient of the tangential supply of a subsonic centripetal turbine]. *Omskiy nauchnyy vestnik. Seriya Aviatsionno-raketnoe i energeticheskoe mashinostroenie*. 2022, Vol. 6, No. 2, P. 78–84 (In Russ.).
14. Idel'chik I. E. *Spravochnik po gidravlicheskim soprotivleniyam* [Handbook of Hydraulic Resistance]. Moscow, Mashinostroenie Publ., 1992, 672 p.
15. Kishkin A. A., Shevchenko Yu. N., Delkov A. V. Analysis of the key design features of low-power turbines for electricity generation. *IOP Conference Series: Materials Science and Engineering*. 2020, Vol. 919, P. 062030. Doi: 10.1088/1757-899X/919/6/062030.
16. Zuev A. A., Kishkin A. A., Zhuikov D. A. et al. Energy equations for the temperature three-dimensional boundary layer for the flow within boundary conditions of turbo machinery. *IOP Conference Series: Materials Science and Engineering*. 2019, vol. 537, P. 22008. Doi: 10.1088/1757-899X/537/2/022008.
17. Karman Th. Uber laminare und turbulente Reibung. *ZAAM*. 1921, No. 1, P. 233–252.

© Shevchenko Yu. N., Kishkin A. A., Zuev A. A., Delkov A. V., Zhuikov D. A., 2024

Шевченко Юлия Николаевна – аспирант; Сибирский государственный университет науки и технологий имени академика М. Ф. Решетнева. E-mail: gift_23j@mail.ru.

Кишкин Александр Анатольевич – доктор технических наук, профессор, заведующий кафедрой холодильной, криогенной техники и кондиционирования; Сибирский государственный университет науки и технологий имени академика М. Ф. Решетнева. E-mail: spsp99@mail.ru.

Зуев Александр Александрович – доктор технических наук, профессор, заведующий кафедрой двигателей летательных аппаратов; Сибирский государственный университет науки и технологий имени академика М. Ф. Решетнева. E-mail: dla2011@inbox.ru.

Делков Александр Викторович – кандидат технических наук, доцент кафедры холодильной, криогенной техники и кондиционирования; Сибирский государственный университет науки и технологий имени академика М. Ф. Решетнева. E-mail: delkov-mx01@mail.ru.

Жуйков Дмитрий Александрович – кандидат технических наук, доцент, доцент кафедры двигателей летательных аппаратов; Сибирский государственный университет науки и технологий имени академика М. Ф. Решетнева. E-mail: dimitri_z@inbox.ru.

Shevchenko Yulia Nikolaevna – post-graduate student; Reshetnev Siberian State University of Science and Technology. E-mail: gift_23j@mail.ru.

Kishkin Alexander Anatolyevich – Dr. Sc., Professor, Head of the Department of Refrigeration, Cryogenic Engineering and Air Conditioning; Reshetnev Siberian State University of Science and Technology. E-mail: spsp99@mail.ru.

Zuev Alexander Alexandrovich – Dr. Sc., Professor, Head of the Department Aircraft Engines; Reshetnev Siberian State University of Science and Technology. E-mail: dla2011@inbox.ru.

Delkov Alexander Viktorovich – Cand. Sc., Associate Professor of the Department of Refrigeration, Cryogenic Engineering and Air Conditioning; Reshetnev Siberian State University of Science and Technology. E-mail: delkov-mx01@mail.ru.

Zhuikov Dmitry Alexandrovich – Cand. Sc., Associate Professor, Associate Professor of the Department of Aircraft Engines; Reshetnev Siberian State University of Science and Technology. E-mail: dimitri_z@inbox.ru.
